

Geophysical Research Letters[®]



RESEARCH LETTER

10.1029/2023GL104803

North Atlantic Tropical Cyclone Intensification: Regional Drivers and Trends

Sharanya J. Majumdar¹ , Samantha Nebylitsa¹ , Philip J. Klotzbach² , Cameron Masiello¹ , and Zachary R. Michael¹

¹Department of Atmospheric Sciences, University of Miami, Miami, FL, USA, ²Department of Atmospheric Science, Colorado State University, Fort Collins, CO, USA

Key Points:

- Atlantic basin rapid intensification trends vary by region, with the greatest increases between 1980–2000 and 2001–2021 south of 22°N
- Wind shear, sea surface temperature, and radius of maximum winds are useful discriminators between intensification rates
- Storm-relative environmental variable trends vary by region, with sea surface temperatures often related to regional intensity change trends

Supporting Information:

Supporting Information may be found in the online version of this article.

Correspondence to:

S. J. Majumdar,
s.majumdar@miami.edu

Citation:

Majumdar, S. J., Nebylitsa, S., Klotzbach, P. J., Masiello, C., & Michael, Z. R. (2023). North Atlantic tropical cyclone intensification: Regional drivers and trends. *Geophysical Research Letters*, 50, e2023GL104803. <https://doi.org/10.1029/2023GL104803>

Received 5 JUN 2023
Accepted 15 AUG 2023

Author Contributions:

Conceptualization: Sharanya J. Majumdar, Samantha Nebylitsa, Philip J. Klotzbach, Cameron Masiello, Zachary R. Michael
Data curation: Sharanya J. Majumdar, Samantha Nebylitsa
Formal analysis: Sharanya J. Majumdar, Samantha Nebylitsa
Funding acquisition: Sharanya J. Majumdar
Investigation: Sharanya J. Majumdar, Samantha Nebylitsa, Philip J. Klotzbach, Cameron Masiello, Zachary R. Michael

Abstract Using 42 years of reanalysis data, we investigate regional, storm-relative characteristics of three groups of Atlantic tropical cyclone intensification: slightly, moderately, and rapidly intensifying. Probability density functions are distinct between these groups for vertical wind shear, sea surface temperature (SST), and radius of maximum winds (RMW), but less so for relative humidity (RH). In the Gulf of Mexico and southern North Atlantic, shear and RMW are good predictors. In the open Atlantic, north of 22°N, shear and SST are the best predictors. In the Caribbean, weaker relationships suggest low statistical predictability in a region where RI cases increased between 1980–2000 and 2001–2021. Of our storm-relative variables tested, increasing SST appears to be most closely connected to the 36% increase in rapidly intensifying events between the two periods, whereas shear and RH are not significantly more favorable. The variability across regions, periods, and variables motivates further investigation.

Plain Language Summary Although many damaging Atlantic tropical cyclones intensify rapidly during their lifetime, forecasting how rapidly they will intensify remains difficult. To address this, we need to better understand whether the conditions in a storm's environment can help identify whether it will intensify rapidly or more slowly, and whether these results change in different regions. Using 42 years of data, we find that wind shear (change in wind speed and direction with height) and ocean temperature are useful to discriminate whether a storm may intensify rapidly versus slowly across the basin, although there is variability in the results. Humidity is less useful. Our results vary by region. The Caribbean shows lower discrimination between intensification rates, highlighting potential difficulties in predicting intensification in this region. This is concerning since the number of rapidly intensifying events has risen sharply in the Caribbean between 1980–2000 and 2001–2021. We also find that the trends in intensifying storms during these 21-year periods vary by region. The most consistent signal related to the rise in intensifying events is the increasing ocean temperature.

1. Introduction

Tropical cyclone (TC) intensification, and especially rapid intensification (RI, 30 kt 24 hr⁻¹) (Kaplan & DeMaria, 2003), remains a key challenge for researchers, forecasters, and decision-makers. Of the 30 North Atlantic (hereafter Atlantic) hurricanes that caused more than \$5 billion in Consumer Price-Adjusted damage in the United States since 1980 (NCEI, 2023), 25 underwent RI. In this paper, we focus on intensifying TCs in the Atlantic basin.

The Statistical Hurricane Intensity Prediction Scheme RI Index (SHIPS-RII; Kaplan et al., 2015) uses a combination of environmental and internal structure predictors to yield probabilistic RI predictions. Statistical relationships between environmental conditions for RI versus slower intensification have been investigated by Hendricks et al. (2010), Wang and Jiang (2021), and Richardson et al. (2022). The first two studies found wind shear, relative humidity (RH), and SST to be useful discriminators, whereas the third used analog TC pairs to identify other variables such as surface latent heat flux. Additional studies suggested a relationship between the radius of maximum winds (RMW) and intensification rate (e.g., Li et al., 2022; Ooyama, 1969; Schubert et al., 2016; Xu & Wang, 2015). Complementing these studies are many observational and modeling studies that investigate inner-core and environmental interactions (e.g., Alvey et al., 2020; DesRosiers et al., 2022; Hazelton et al., 2020; Rios-Berrios et al., 2018; Ryglicki et al., 2019).

Several studies have also noted a recent increase in Atlantic RI events. Balaguru et al. (2018) found an increasing trend in the central and eastern Atlantic between 1986 and 2015, and Bhatia et al. (2019) found an increasing

© 2023. The Authors.

This is an open access article under the terms of the [Creative Commons Attribution-NonCommercial-NoDerivs License](https://creativecommons.org/licenses/by/4.0/), which permits use and distribution in any medium, provided the original work is properly cited, the use is non-commercial and no modifications or adaptations are made.

Methodology: Sharanya J. Majumdar, Samantha Nebylitsa, Philip J. Klotzbach, Cameron Masiello, Zachary R. Michael

Project Administration: Sharanya J. Majumdar

Resources: Sharanya J. Majumdar

Software: Sharanya J. Majumdar, Samantha Nebylitsa, Cameron Masiello, Zachary R. Michael

Supervision: Sharanya J. Majumdar, Philip J. Klotzbach

Validation: Sharanya J. Majumdar, Samantha Nebylitsa

Visualization: Sharanya J. Majumdar, Samantha Nebylitsa

Writing – original draft: Sharanya J. Majumdar, Philip J. Klotzbach

Writing – review & editing: Sharanya J. Majumdar, Samantha Nebylitsa, Philip J. Klotzbach, Cameron Masiello, Zachary R. Michael

basinwide trend between 1982 and 2009. Klotzbach et al. (2022) found an increasing (albeit insignificant) trend between 1990 and 2021. These trends have also been examined together with trends in relevant environmental variables. Bhatia et al. (2022) found that the probability of RI increased as more threshold values of TC-relative environmental variables were exceeded. Balaguru et al. (2022) investigated regional trends in near-shore variables, suggesting an increasingly favorable dynamic and thermodynamic environment for intensification.

Given that atmospheric and oceanic features vary across the Atlantic basin, TC intensification rates and their relationships with environmental variables may also vary by region. Their trends may vary by region too, and there is scope to build on Balaguru et al. (2018, 2022) and Bhatia et al. (2022) to reveal new regional relationships. To date, no studies have investigated observed regional trends using probability density functions (PDFs) of TC-relative environmental variables, for RI versus slower intensification.

In this study, we use best track and reanalysis datasets from 1980 to 2021 to investigate three related issues within the Atlantic basin and four sub-regions. First, we compare RI trends against moderate intensification (MI, 15–25 kt 24 hr⁻¹) and slight intensification (SI, 5–10 kt 24 hr⁻¹), between 1980–2000 and 2001–2021. Next, for the full 42-year period, we compute PDFs to evaluate the differences between distributions of TC-relative environmental variables for RI, MI, and SI. Finally, we aim to reconcile changes in intensification rate frequency with corresponding changes in the PDFs of the environmental variables over the two 21-year periods.

2. Data and Methodology

Our sample comprises all Atlantic TCs between 1980 and 2021, using the National Hurricane Center Best Track database (HURDAT2, Landsea & Franklin, 2013) and, for RMW only, the extended best track (Demuth et al., 2006) from 1988. Before 2021, RMW values were not reanalyzed post-storm (Chavas & Knaff, 2022), and some records in 1988–1989 are missing. Both datasets are six-hourly, and the intensification rate refers to the increase in intensity in the 24 hr subsequent to each time. Using this convention, a TC may undergo multiple intensification events during its lifetime. We calculate intensification rates at any point when the TC is at least at tropical depression intensity. To date, intensification trend analysis has mostly used the International Best-Track Archive for Climate Stewardship (IBTrACS, Knapp et al., 2010) which includes HURDAT2 as its Atlantic input source. Due to advances in satellite and aircraft observations during our analysis period, the quality of best track estimates of intensity and RMW is temporally inhomogeneous. To address this, Bhatia et al. (2019) compared intensification rates from IBTrACS with those from the more temporally homogeneous Advanced Dvorak Technique-Hurricane Satellite-B1 (ADT-HURSAT, Kossin et al., 2013) during 1982–2017, and concluded that the agreement between the two datasets provided confidence in their Atlantic basin trend analysis. To remain consistent with Balaguru et al. (2018, 2020, 2022) and Bhatia et al. (2018, 2019, 2022), our analysis uses best track data. Estimates of intensity and RMW uncertainty are provided in Landsea and Franklin (2013) and Landsea (2022), respectively. These uncertainties vary with intensity and availability of aircraft and satellite data.

To compute TC-relative environmental variables, we use six-hourly data from the European Centre for Medium-Range Weather Forecasts version 5 reanalysis data set (ERA5; Hersbach et al., 2020) on a 0.25° grid. Our variables are the magnitude of the 200–850 hPa vertical wind shear averaged within an annulus of 200–800 km from the TC center (hereafter referred to as “shear”), 500–700 hPa average RH using the same annulus, and SST at the ERA5 grid point nearest to the TC center. The shear and RH definitions are the same as those used in DeMaria et al. (2005). There are caveats in the use of ERA5 data to investigate TC environments and trends, due to changes and limitations in the observing network along with the global model and data assimilation. Some of these limitations have been evaluated by Slocum et al. (2022) for 1998–2019. First, the mean (standard deviation) position offsets from the best track have decreased from ~75 to 50 km (~50–25 km). We expect that the mean value may exceed 100 km prior to 1998. They estimated that these position errors would lead to a mean absolute deviation of shear of 0.8 kt. Next, they found ERA5 shear (RH) to be <0.5 kt lower (2% drier) than in SHIPS. Due to these published uncertainties and the arguments of Balaguru et al. (2022), Bhatia et al. (2022), and Richardson et al. (2022) who used ERA5, we suggest that there are no known large trends that will skew our PDFs.

We compute PDFs of each variable, for subsets grouped by intensification rate (RI, MI, SI), and 21-year period. We use non-parametric Kolmogorov-Smirnov (K-S) tests to evaluate the difference in two PDFs, via the maximum “distance” between their respective cumulative distribution functions. The p-value refers to the probability that the distance is greater than the computed value and is computed using the Python statistics

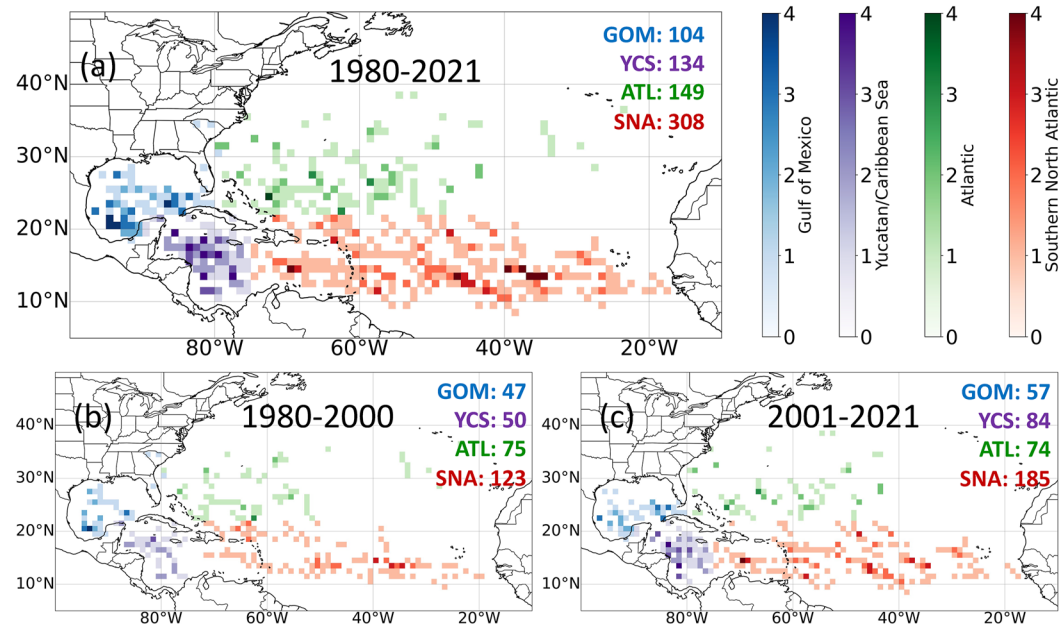


Figure 1. Geographical distribution of Atlantic rapid intensification (RI) events. (a) 1980–2021, (b) 1980–2000, and (c) 2001–2021. The numbers of RI events for each period in each color-coded region are provided.

package “scipy.stats.ks_2samp,” using methods from Hodges (1958). For ease of interpretation, we use $\alpha = -\log_{10}(p\text{-value})$, with values exceeding 1.3, 2.0, and 3.0 demonstrating statistically significant differences at 5%, 1%, and 0.1% respectively. Larger values of α correspond to greater differences between distributions. We compare relative values of α ; for example, the α values of RI versus MI.

3. Regional and Temporal Intensification Rate Characteristics

We divide the Atlantic basin into four regions, color-coded in Figure 1:

- Gulf of Mexico (GOM): $>22^{\circ}\text{N}$ and 80°W – 90°W inclusive and all latitudes $<90^{\circ}\text{W}$;
- Yucatan/western Caribbean Sea (YCS): $\leq 22^{\circ}\text{N}$, 75°W – 90°W exclusive;
- Atlantic (ATL): $>22^{\circ}\text{N}$, $>80^{\circ}\text{W}$;
- South N. Atlantic (SNA): $\leq 22^{\circ}\text{N}$, $\geq 75^{\circ}\text{W}$.

The locations at which all RI, MI, and SI events were initiated between 1980 and 2021 are illustrated in Figure 1; Figures S1 and S2 in Supporting Information S1 respectively, with the number of cases listed on the figures and in Table S1 in Supporting Information S1. 34% of the RI events occurred in the GOM and YCS (Figure 1a), compared with 26% of the MI events and 20% of the SI events, indicating the propensity for TCs to intensify at faster rates in the western Atlantic. Comparing 1980–2000 versus 2001–2021 (Figures 1b and 1c), the basinwide number of RI events has increased by 36%. The number of TCs per year undergoing RI increased from 4.3 to 4.8, and the number of RI events per TC increased from 3.3 to 4.0. This suggests that the basinwide increase is related to the number of TCs undergoing RI and the lengthening of the RI process. In the YCS, the increase in RI (68%) and MI (75%) events is larger. In the SNA, the increase in RI events is 50%, much higher than the increases in MI and SI events. In the ATL, there is no trend in RI events, whereas there is a 29% increase in MI and SI events.

4. Basinwide PDFs of Environmental Variables

We now investigate whether the full sample reveals distinct differences in the four variables (shear, RH, SST, RMW) between the three intensification rates (RI, MI, SI), using PDFs of each variable normalized by sample size (Figure 2).

For shear, K-S testing reveals that each pair of intensification rates yields statistically distinct distributions, with a large distinction between RI and MI ($\alpha = 10.3$, Table S2 in Supporting Information S1). Additional information

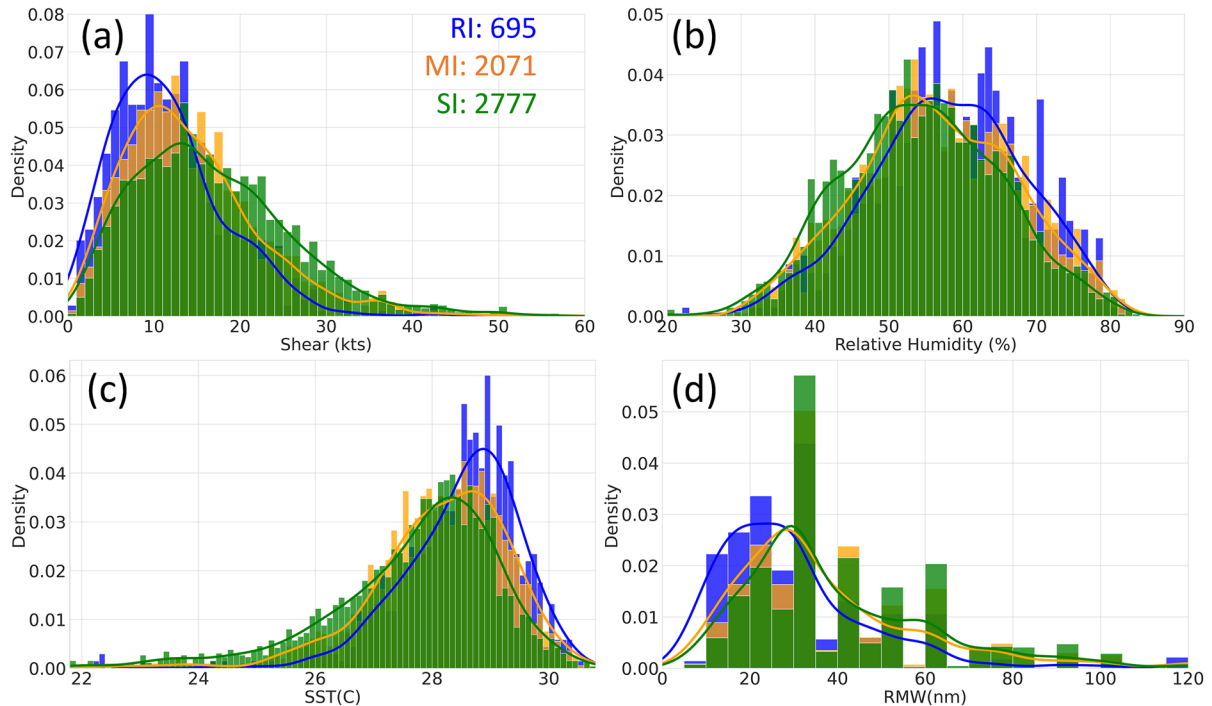


Figure 2. Environmental and structural conditions associated with intensifying Atlantic TCs between 1980 and 2021. Probability density functions of (a) shear, (b) relative humidity, (c) sea surface temperature, and (d) radius of maximum winds (RMW), for (blue) rapid intensification, (orange) moderate intensification, and (green) slight intensification. Several outlying values for RMW > 120 nm have been excluded in panel (d) to focus on key relationships. The number of cases is listed in (a). RMW data are available from 1988.

can be gleaned from the PDFs (Figure 2a). First, the mode, median, and PDF shift toward increasing values for slower intensification, consistent with the larger average shear found by Hendricks et al. (2010) and Wang and Jiang (2021). The peaks for RI and MI are sharper than that for SI, suggesting that SI occurs over a broader range of shear values. For RI, there is a greater density for low shear, compared with MI and especially SI. While the density of high shear is lower for RI, 10% of all RI events still occurred in shear >21 kt. For moderate shear (~15 kt), there is no preferred intensification rate, with their PDF values approximately equal.

In contrast, the relationship for RH is less clear (Figure 2b), with the statistical significance between RI and MI being the lowest of all pairs of PDFs ($\alpha = 2.9$) over all four variables. However, some spikes in the PDF for RH > 60% in the RI category are evident. RI can also occur when the RH is low, with 10% of all RI cases occurring when RH < 45%. Our finding that RH is a more marginal discriminant between intensification rates than for shear is consistent with Hendricks et al. (2010) and Knaff et al. (2018). However, Wang and Jiang (2021) found significantly larger RH for RI events versus slower intensifiers using the SHIPS database. In RI forecasting, while SHIPS and other aids (e.g., Knaff et al., 2018) have an RH component, SHIPS RII does not. Our results do not provide a compelling argument to include RH.

SST is statistically a strong discriminator between RI and MI (Figure 2c, $\alpha = 9.5$), with the RI PDF shifted toward higher SST by 0.2–0.3°C and a substantially higher concentration of values >28.5°C. Our findings are consistent with Hendricks et al. (2010) and Wang and Jiang (2021) who identified similar average differences in SST between RI and slower intensifiers.

The RMW is also a significant discriminant between RI and MI (Figure 2d, $\alpha = 12.2$). 25% of all RI cases occur when the RMW is between 5 and 15 nm (inclusive). In contrast, the corresponding fraction of non-rapid (5–25 kt) intensifications with an initial RMW between 5 and 15 nm is only 12%. There is only a relatively small degree of discrimination between MI and SI.

Given that the RMW depends on the TC's initial intensity (e.g., Chavas & Knaff, 2022), we investigate whether a significant relationship exists between the RMW and the subsequent 24-hr intensification rate. Using subsamples of RI and MI TCs stratified by intensity (25–30 kt, 35–40 kt, ..., 125–130 kt), a decreasing relationship is found

for each subsample between 35 and 80 kt. The Pearson correlation coefficient r varies between -0.12 and -0.19 in these subsamples, corresponding to $>95\%$ statistical significance. Hence, we hypothesize that the relationship between RMW and intensification rate is partially causal.

We finally note the high spread of values in each of the intensification rates, indicating substantial case-by-case variability, and the large overlap between their respective PDFs.

5. Regional PDFs of Environmental Variables

The PDFs are now presented in Figure 3 for the four regions, with K-S values in Table S2 in Supporting Information S1. For shear (Figures 3a–3d), the respective PDFs for RI, MI, and SI shift toward higher values in the GOM, ATL, and SNA, and are statistically distinct, consistent with the basinwide result in Figure 2a. In the GOM (Figure 3a), the PDFs are most distinct, with mode values of 10 kt for RI, 14 kt for MI, and 18 kt for SI. The RI mode ranges from 8 kt in the SNA to 11 kt in the ATL. The fraction of TCs that undergo RI in highly-sheared environments (>20 kt) is largest in the ATL, a result that warrants future investigation. The YCS shows smaller differences between the PDFs for the three intensification rates.

The distinctions between the SST PDFs in each region are intriguing, even though the mode values are narrowly bound between 28 and 29°C (Figures 3e–3h). The range of SSTs in which RI occurs in the ATL is broader than the other three regions, with the 25th percentile of SST in the RI sample being 26.7°C, considerably cooler than the SNA (27.6°C), GOM (28.5°C), and YCS (28.6°C). This result may reflect larger geographical variability in ATL SST. The RI, MI, and SI PDFs are most distinct in the ATL, although RI versus SI is distinct in the GOM and SNA. The PDFs are least distinct in the YCS. A possible reason is that pre-storm SSTs and TC-induced SST cooling vary in phase in the western Atlantic, making SST a less useful predictor in the YCS (Foltz et al., 2018).

These results suggest that in the GOM and SNA, wind shear has a strong bearing on whether RI will occur, whereas in the ATL, both SST and wind shear play an important role. In the YCS, no clear relationships are evident.

No statistically significant distinctions between RI and MI are evident in the RH PDFs (Figures S3a–S3d and Table S2 in Supporting Information S1). The mode of RH for RI varies from 54% (ATL) to 71% (YCS). The PDFs in the western regions (GOM, YCS) exhibit more variability. The ATL, which has the highest mode (and median) of shear, possesses the lowest mode (and median) of RH, and vice versa for the two more southern regions. However, high shear and low RH do not always preclude intensification, even RI, as noted in Bhatia et al. (2022). For RMW, the most significant discrimination between RI and MI is found in the SNA, where TCs forming from African easterly waves may possess compact eyewalls (Figures S3e–S3h in Supporting Information S1). The RMW PDFs also exhibit clear differences in the GOM and ATL. In the YCS, as for shear and SST, the intensification categories for RMW are indistinct.

Regional variations in shear, SST and RH arise due to combinations of tropical (e.g., ENSO, Atlantic Meridional Mode) and extratropical forcing mechanisms (e.g., anticyclonic wave breaking (AWB)). This especially applies to the ATL, with higher shear possible due to the presence of the tropical upper-tropospheric trough and associated AWB (Jones et al., 2020; Wang et al., 2020), and lower RH due to mid-latitude dry air intrusions (Dunion, 2011). Especially for shear and RH, the climatology of TC-relative environmental parameters is expected to differ from the regional climatology of the same parameters. As pointed out by Bhatia et al. (2022), TC-relative parameters are essential to better understand changes at timescales that are most relevant for TC intensification.

6. PDFs of Environmental Variables: 1980–2000 Versus 2001–2021

The K-S values for pairs of intensification categories for each 21-year period, and for pairs of 21-year periods for each intensification category, are provided in Tables S3 and S4 in Supporting Information S1 respectively. The PDFs for the latter pairs, for RI, are illustrated in Figure 4. The shear PDFs are distinct (Figure 4a). The mode in 1980–2000 is 8 kt, while the mode in 2001–2021 is 11 kt. In contrast, the RH PDFs are similar for the 21-year periods (Figure 4b). However, there is a stronger distinction between the RI and MI PDFs for RH in 2001–2021 ($\alpha = 2.4$) than in 1980–2000 ($\alpha = 0.6$) (Table S3 in Supporting Information S1), suggesting that RH may be an important discriminator for intensity change in the 21st century. Finally, the SST PDF has shifted to the right in 2001–2021, with the mean, median, and mode values increasing by 0.3°C (Figure 4c). The SST has

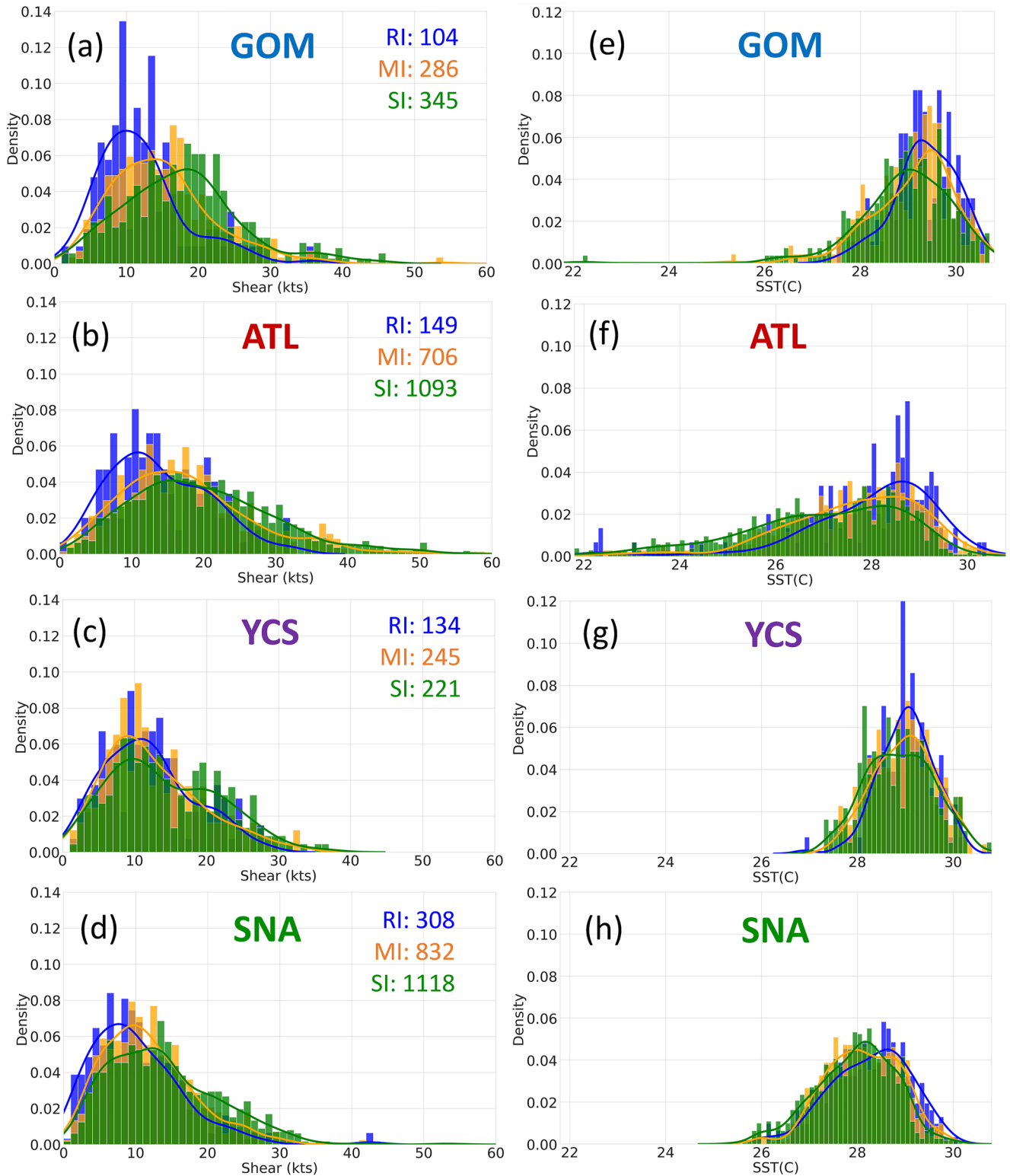


Figure 3. Environmental conditions associated with intensifying Atlantic TCs. Probability density functions of (a–d) shear and (e–h) sea surface temperature for (blue) rapid intensification, (orange) moderate intensification, and (green) slight intensification, for the four regions: Gulf of Mexico, ATL, Yucatan/western Caribbean Sea, and SNA. The number of cases in each region in the 1980–2021 sample is listed in a–d.

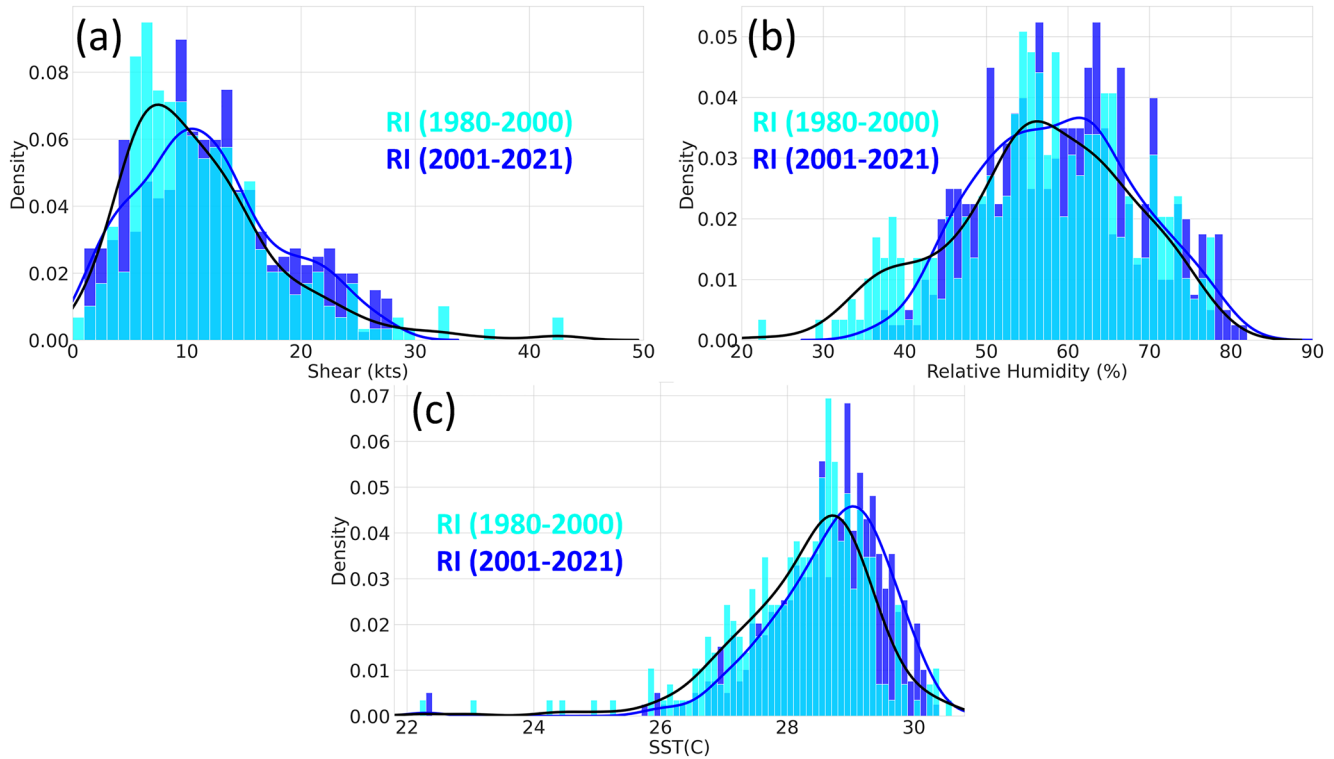


Figure 4. Environmental conditions associated with rapidly-intensifying Atlantic TCs in 1980–2000 and 2001–2020. Probability density functions of (a) shear, (b) relative humidity, and (c) sea surface temperature for 1980–2000 (light blue bars; black line) and 2001–2021 (dark blue bars; dark blue line).

been increasing by 0.1–0.3°C per decade in most portions of the Atlantic basin (Balaguru et al., 2022; Klotzbach et al., 2022), with the change in the open Atlantic hypothesized to be due to a slowdown in the AMOC and an enhanced north Atlantic subtropical high (Balaguru et al., 2022). There is an even greater increase in SST for MI and SI (Table S4 in Supporting Information S1).

In each region, SSTs are increasing for each intensification rate. The most pronounced trend is in the SNA (Table S4 in Supporting Information S1), where there is a 52% increase in RI events (Table S1 in Supporting Information S1). In the SNA, the shear and RH trends are less clear. In the YCS, where RI has increased by >68%, the SST increase is modest, and the shear for RI surprisingly increased. In the ATL, the modest increase in SST is accompanied by increases in RH and shear. The RH PDF shifted slightly toward increasing values in GOM and ATL, north of 22°N. While there are regional variations in the temporal changes in the TC-relative shear and RH, it is not yet clear how they may explain temporal changes in the regional relationships between RI and slower intensification.

7. Concluding Remarks

Using best track and ERA5 reanalysis data in the Atlantic basin between 1980 and 2021, we have examined basinwide and regional differences and trends for TCs undergoing rapid, moderate, and slight intensification, and their relationships with TC-relative variables.

The fraction of RI events is higher west of 75°W, where the SST and RH are generally higher. Over the full basin, there were 36% more RI events in 2001–2021 than in 1980–2000, in keeping with the findings of Balaguru et al. (2018) and Bhatia et al. (2019). The most pronounced regional increases were in the YCS and SNA.

Statistical comparisons between PDFs of the TC-relative variables, separated by intensification rate, revealed that vertical wind shear magnitude and SST were good predictors for RI, consistent with Hendricks et al. (2010) and Wang and Jiang (2021). We found a less clear relationship for RH, as Knaff et al. (2018) found for the western north Pacific. RMW was a good predictor, with smaller TCs more likely to undergo RI, consistent with Xu and Wang (2015) and Knaff et al. (2018).

The PDFs illustrated a high variability of each variable for each intensification rate, with overlap across them. The PDFs allow for more robust interpretations than using averages; for example, the fraction of RI cases that occur in high shear.

The relationships between intensification rate and environmental conditions vary by region. In the GOM, shear and RMW were especially good predictors for RI. In the ATL, where the range of SSTs had the most variability, SST and shear were strong predictors. In the SNA, shear and especially RMW were good predictors. Conversely, except for modest RH utility, the relationships were weak in the YCS. This result is concerning, given that RI events have increased by 68% in the YCS in the early 21st century. We recommend further investigations into why statistical predictability of intensification is low in this region. For RI cases, the ATL had the highest shear mode of shear and the lowest RH mode, with the converse being true for the two southern regions.

The mode of TC-relative vertical wind shear for RI events increased by ~ 3 kt between the two 21-year periods, with the main contributions from the ATL and YCS. This result is inconsistent with Balaguru et al. (2022) who found decreasing shear in the western Atlantic basin, suggesting that results in a TC-relative framework may differ from averages on a fixed grid. The average SST increased by 0.3°C , consistent with Klotzbach et al. (2022) and Balaguru et al. (2022). The corresponding RH PDFs indicated a general increase in TC-relative RH north of 22°N . Overall, while some regional variations in the trends of shear and RH were evident, we suggest that the TC-relative variable most responsible for the increase in RI events is SST.

The study contains several caveats. Observational advances in recent decades may be responsible for a portion of the observed RI increase. There are also uncertainties in ERA5 data near TCs (Slocum et al., 2022), and these uncertainties vary not only with time but also with data coverage near each TC (e.g., aircraft and satellite). Although ERA5 is state-of-the-art at the time of this study, future improved reanalyses may yield results that differ slightly from ours. Our sample is dominated by TCs with many RI episodes, although results that only include the first onset of RI are similar (Nebylitsa et al., 2023). The Kolmogorov-Smirnov test is not a comprehensive test of the discrimination between two PDFs.

Other variables might be more robust predictors of intensity change in some regions. Examples include salinity (Balaguru et al., 2020), potential intensity (Balaguru et al., 2022; Bhatia et al., 2022; DeMaria, 2009), ventilation index (Tang & Emanuel, 2012), and forward motion (Hendricks et al., 2010; Kaplan & DeMaria, 2003). Our RMW result emphasizes the inclusion of internal TC characteristics. We have only examined our variables individually, and next steps involve identifying combinations (e.g., Bhatia et al., 2022) using joint PDFs. The results may also vary by month and basin (Wang & Jiang, 2021). Although we estimated shear and RH based on the SHIPS definitions, the results may vary with different variable definitions (Nebylitsa et al., 2023). Detailed investigations are required to shed light on these results, including the atmospheric and oceanographic reasoning behind the regional differences between the PDFs of the TC-relative variables. A full analysis of the trends in the TC-relative variables will yield further insights. We also encourage the introduction of statistical forecasting techniques that account for the full PDFs.

Data Availability Statement

Most TC data were taken from the International Best Track Archive for Climate Stewardship version 4: <https://www.ncei.noaa.gov/products/international-best-track-archive>. The extended best track is available at: https://rammb2.cira.colostate.edu/research/tropical-cyclones/tc_extended_best_track_dataset/. All atmospheric and oceanic data were obtained from ERA5 reanalysis: <https://www.ecmwf.int/en/forecasts/dataset/ecmwf-reanalysis-v5>.

References

- Alvey, G. R., Zipser, E., & Zawislak, J. (2020). How does hurricane Edouard (2014) evolve toward symmetry before rapid intensification? A high-resolution ensemble study. *Journal of the Atmospheric Sciences*, 77(4), 1329–1351. <https://doi.org/10.1175/JAS-D-18-0355.1>
- Balaguru, K., Foltz, G. R., & Leung, L. R. (2018). Increasing magnitude of hurricane rapid intensification in the eastern and central tropical Atlantic. *Geophysical Research Letters*, 45(9), 4238–4247. <https://doi.org/10.1029/2018GL077597>
- Balaguru, K., Foltz, G. R., Leung, L. R., Kaplan, J., Xu, W., Reul, N., & Chapron, B. (2020). Pronounced impact of salinity on rapidly intensifying tropical cyclones. *Bulletin of the American Meteorological Society*, 101(9), E1497–E1511. <https://doi.org/10.1175/BAMS-D-19-0303.1>
- Balaguru, K., Foltz, G. R., Leung, L. R., Xu, W., Kim, D., Lopez, H., & West, R. (2022). Increasing hurricane intensification rate near the US Atlantic coast. *Geophysical Research Letters*, 49(20), e2022GL099793. <https://doi.org/10.1029/2022GL099793>
- Bhatia, K., Baker, A., Yang, W., Vecchi, G., Knutson, T., Murakami, H., et al. (2022). A potential explanation for the global increase in tropical cyclone rapid intensification. *Nature Communications*, 13(1), 6626. <https://doi.org/10.1038/s41467-022-34321-6>

Acknowledgments

S. Majumdar, S. Nebylitsa, C. Masiello, and Z. Michael acknowledge support from ONR TCRI Grant N00014-20-1-2075, and P. Klotzbach was supported by the G. Unger Vetlesen Foundation and ONR TCRI Grant N00014-20-1-2069. We thank C. Slocum, two anonymous reviewers, J. Cangialosi, C. Landsea, B. McNoldy, D. Nolan, and J. Zawislak for helpful suggestions.

- Bhatia, K., Vecchi, G., Murakami, H., Underwood, S., & Kossin, J. (2018). Projected response of tropical cyclone intensity and intensification in a global climate model. *Journal of Climate*, *31*(20), 8281–8303. <https://doi.org/10.1175/JCLI-D-17-0898.1>
- Bhatia, K. T., Vecchi, G. A., Knutson, T. R., Murakami, H., Kossin, J., Dixon, K. W., & Whitlock, C. E. (2019). Recent increases in tropical cyclone intensification rates. *Nature Communications*, *10*(1), 1–9. <https://doi.org/10.1038/s41467-019-08471-z>
- Chavas, D. R., & Knaff, J. A. (2022). A simple model for predicting the tropical cyclone radius of maximum wind from outer size. *Weather and Forecasting*, *37*(5), 563–579. <https://doi.org/10.1175/WAF-D-21-0103.1>
- DeMaria, M. (2009). A simplified dynamical system for tropical cyclone intensity prediction. *Monthly Weather Review*, *137*(1), 68–82. <https://doi.org/10.1175/2008MWR2513.1>
- DeMaria, M., Mainelli, M., Shay, L. K., Knaff, J. A., & Kaplan, J. (2005). Further improvements to the statistical Hurricane intensity prediction scheme (SHIPS). *Weather and Forecasting*, *20*(4), 531–543. <https://doi.org/10.1175/WAF862.1>
- Demuth, J. L., DeMaria, M., & Knaff, J. A. (2006). Improvement of advanced microwave sounding unit tropical cyclone intensity and size estimation algorithms. *Journal of Applied Meteorology and Climatology*, *45*(11), 1573–1581. <https://doi.org/10.1175/JAM2429.1>
- DesRosiers, A. J., Bell, M. M., & Cha, T. (2022). Vertical vortex development in Hurricane Michael (2018) during rapid intensification. *Monthly Weather Review*, *150*(1), 99–114. <https://doi.org/10.1175/MWR-D-21-0098.1>
- Dunion, J. P. (2011). Rewriting the climatology of the tropical North Atlantic and Caribbean Sea atmosphere. *Journal of Climate*, *24*(3), 893–908. <https://doi.org/10.1175/2010JCLI3496.1>
- Foltz, G. R., Balaguru, K., & Hagos, S. (2018). Interbasin differences in the relationship between SST and tropical cyclone intensification. *Monthly Weather Review*, *146*(3), 853–870. <https://doi.org/10.1175/MWR-D-17-0155.1>
- Hazelton, A. T., Zhang, X., Gopalakrishnan, S., Ramstrom, W., Marks, F., & Zhang, J. A. (2020). High-resolution ensemble HFV3 forecasts of Hurricane Michael (2018): Rapid intensification in shear. *Monthly Weather Review*, *148*(5), 2009–2032. <https://doi.org/10.1175/MWR-D-19-0275.1>
- Hendricks, E. A., Peng, M. S., Fu, B., & Li, T. (2010). Quantifying environmental control on tropical cyclone intensity change. *Monthly Weather Review*, *138*(8), 3243–3271. <https://doi.org/10.1175/2010MWR3185.1>
- Hersbach, H., Bell, B., Berrisford, P., Hirahara, S., Horanyi, A., Munoz-Sabater, J., et al. (2020). The ERA5 global reanalysis. *Quarterly Journal of the Royal Meteorological Society*, *146*(730), 1999–2049. <https://doi.org/10.1002/qj.3803>
- Hodges, J. L., Jr. (1958). The significance probability of the Smirnov two-sample test. *Arkiv för Matematik*, *3*(5), 469–486. <https://doi.org/10.1007/bf02589501>
- Jones, J. J., Bell, M. M., & Klotzbach, P. J. (2020). Tropical and Subtropical North Atlantic vertical wind shear and seasonal tropical cyclone activity. *Journal of Climate*, *33*(13), 5413–5426. <https://doi.org/10.1175/JCLI-D-19-0474.1>
- Kaplan, J., & DeMaria, M. (2003). Large-scale characteristics of rapidly intensifying tropical cyclones in the North Atlantic basin. *Weather and Forecasting*, *18*(6), 1093–1108. [https://doi.org/10.1175/1520-0434\(2003\)018%3C1093:LCORIT%3E2.0.CO;2](https://doi.org/10.1175/1520-0434(2003)018%3C1093:LCORIT%3E2.0.CO;2)
- Kaplan, J., Rozoff, C. M., DeMaria, M., Sampson, C. R., Kossin, J. P., Velden, C. S., et al. (2015). Evaluating environmental impacts on tropical cyclone rapid intensification predictability using statistical models. *Weather and Forecasting*, *30*(5), 1374–1396. <https://doi.org/10.1175/WAF-D-15-0032.1>
- Klotzbach, P. J., Wood, K. M., Schreck, C. J., Bowen, S. G., Patricola, C. M., & Bell, M. M. (2022). Trends in global tropical cyclone activity: 1990–2021. *Geophysical Research Letters*, *49*(6), e2021GL095774. <https://doi.org/10.1029/2021GL095774>
- Knaff, J. A., Sampson, C. R., & Musgrave, K. D. (2018). An operational rapid intensification prediction aid for the western North Pacific. *Weather and Forecasting*, *33*(3), 799–811. <https://doi.org/10.1175/WAF-D-18-0012.1>
- Knapp, K. R., Kruk, M. C., Levinson, D. H., Diamond, H. J., & Neumann, C. J. (2010). The international best track archive for climate stewardship (IBTrACS). *Bulletin of the American Meteorological Society*, *91*(3), 363–376. <https://doi.org/10.1175/2009BAMS2755.1>
- Kossin, J. P., Olander, T. L., & Knapp, K. R. (2013). Trend analysis with a new global record of tropical cyclone intensity. *Journal of Climate*, *26*(24), 9960–9976. <https://doi.org/10.1175/JCLI-D-13-00262.1>
- Landsea, C. W. (2022). The revised Atlantic hurricane database (HURDAT2). Retrieved from <https://www.nhc.noaa.gov/data/hurdat/hurdat2-format-atl-1851-2021.pdf>
- Landsea, C. W., & Franklin, J. L. (2013). Atlantic hurricane database uncertainty and presentation of a new database format. *Monthly Weather Review*, *141*(10), 3576–3592. <https://doi.org/10.1175/MWR-D-12-00254.1>
- Li, Y., Wang, Y., & Tan, Z.-M. (2022). Why does the initial wind profile inside the radius of maximum wind matter to tropical cyclone development? *Journal of Geophysical Research: Atmospheres*, *127*(16), e2022JD037039. <https://doi.org/10.1029/2022JD037039>
- NOAA National Centers for Environmental Information (NCEI). (2023). US billion-dollar weather and climate disasters. <https://doi.org/10.25921/stkw-7w73>
- Nebylitsa, S., Majumdar, S. J., & Nolan, D. S. (2023). Revisiting environmental wind and moisture calculations in the context of tropical cyclone intensification. *Weather and Forecasting*. In Press. <https://doi.org/10.1175/WAF-D-23-0045.1>
- Ooyama, K. (1969). Numerical simulation of the life cycle of tropical cyclones. *Journal of the Atmospheric Sciences*, *26*(1), 3–40. [https://doi.org/10.1175/1520-0469\(1969\)026<0003:NSOTLC>2.0.CO;2](https://doi.org/10.1175/1520-0469(1969)026<0003:NSOTLC>2.0.CO;2)
- Richardson, J. C., Torn, R. D., & Tang, B. H. (2022). An analog comparison between rapidly and slowly intensifying tropical cyclones. *Monthly Weather Review*, *150*(8), 2139–2156. <https://doi.org/10.1175/MWR-D-21-0260.1>
- Rios-Berrios, R., Davis, C. A., & Torn, R. D. (2018). A hypothesis for the intensification of tropical cyclones under moderate vertical wind shear. *Journal of the Atmospheric Sciences*, *75*(12), 4149–4173. <https://doi.org/10.1175/JAS-D-18-0070.1>
- Ryglicki, D. R., Doyle, J. D., Hodyss, D., Cossuth, J. H., Jin, Y., Viner, K. C., & Schmidt, J. M. (2019). The unexpected rapid intensification of tropical cyclones in moderate vertical wind shear. Part III: Outflow–environment interaction. *Monthly Weather Review*, *147*(8), 2919–2940. <https://doi.org/10.1175/MWR-D-18-0370.1>
- Schubert, W. H., Slocum, C. J., & Taft, R. K. (2016). Forced, balanced model of tropical cyclone intensification. *Journal of the Meteorological Society of Japan*, *94*(2), 119–135. <https://doi.org/10.2151/jmsj.2016-007>
- Slocum, C. J., Razin, M. N., Knaff, J. A., & Stow, J. P. (2022). Does ERA5 mark a new era for resolving the tropical cyclone environment? *Journal of Climate*, *35*(21), 3547–3564. <https://doi.org/10.1175/JCLI-D-22-0127.1>
- Tang, B., & Emanuel, K. (2012). A ventilation index for tropical cyclones. *Bulletin of the American Meteorological Society*, *93*(12), 1901–1912. <https://doi.org/10.1175/BAMS-D-11-00165.1>
- Wang, X., & Jiang, H. (2021). Contrasting behaviors between the rapidly intensifying and slowly intensifying tropical cyclones in the North Atlantic and eastern Pacific basins. *Journal of Climate*, *34*(3), 987–1003. <https://doi.org/10.1175/JCLI-D-19-0908.1>

- Wang, Z., Zhang, G., Dunkerton, T. J., & Jin, F.-F. (2020). Summertime stationary waves integrate tropical and extratropical impacts on tropical cyclone activity. *Proceedings of the National Academy of Sciences of the United States of America*, *117*(37), 22720–22726. <https://doi.org/10.1073/pnas.2010547117>
- Xu, J., & Wang, Y. (2015). A statistical analysis on the dependence of tropical cyclone intensification rate on the storm intensity and size in the North Atlantic. *Weather and Forecasting*, *30*(3), 692–701. <https://doi.org/10.1175/WAF-D-14-00141.1>